Late-summer carbon fluxes from Canadian forests and peatlands along an east–west continental transect

Carole Coursolle, Hank A. Margolis, Alan G. Barr, T. Andrew Black, Brian D. Amiro, J. Harry McCaughey, Lawrence B. Flanagan, Peter M. Lafleur, Nigel T. Roulet, Charles P.-A. Bourque, M. Altaf Arain, Steven C. Wofsy, Allison Dunn, Kai Morgenstern, Alberto L. Orchansky, Pierre Y. Bernier, Jing M. Chen, Joe Kidston, Nobuko Saigusa, and Newell Hedstrom

Abstract: Net ecosystem productivity (NEP) during August 2003 was measured by using eddy covariance above 17 forest and 3 peatland sites along an east–west continental-scale transect in Canada. Measured sites included recently disturbed stands, young forest stands, intermediate-aged conifer stands, mature deciduous stands, mature conifer stands, fens, and an open shrub bog. Diurnal courses of NEP showed strong coherence within the different ecosystem categories. Recently disturbed sites showed the weakest diurnal cycle; and intermediate-aged conifers, the strongest. The western treed fen had a more pronounced diurnal pattern than the eastern shrub bog or the Saskatchewan patterned fen. All but three sites were clearly afternoon C sinks. Ecosystem respiration was highest for the young fire sites. The intermediate-aged conifer sites had the highest maximum NEP (NEP_{max}) and gross ecosystem productivity (GEP_{max}), attaining rates that would be consistent with the presence of a strong terrestrial C sink in regions where these types of forest are common. These results support the idea that large-scale C cycle modeling activities would benefit from information on the age-class distribution and disturbance types within larger grid cells. Light use efficiency followed a pattern similar to that of NEP_{max} and GEP_{max}. Four of the five recently disturbed sites and all three of the peatland sites had low water use efficiencies.

Résumé : La productivité nette des écosystèmes (PNE) au cours du mois d'août 2003 a été mesurée à l'aide de la méthode de covariance des turbulences au-dessus de 17 forêts et de 3 tourbières réparties le long d'un transect est–ouest transcontinental au Canada. Les stations mesurées incluent des peuplements récemment perturbés, de jeunes peuplements

Received 5 April 2005. Accepted 10 November 2005. Published on the NRC Research Press Web site at http://cjfr.nrc.ca on 22 March 2006.

C. Coursolle and H.A. Margolis.[1] Faculté de foresterie et de géomatique, Pavillon Abitibi-Price, Université Laval, Québec, QC G1K 7P4, Canada.
A.G. Barr. Climate Research Branch, Meteorological Service of Canada, 11 Innovation Boulevard, Saskatoon, SK S7N 3H5, Canada.
T.A. Black, K. Morgenstern, and J. Kidston. Faculty of Agricultural Sciences, 135-2357 Main Mall, The University of British Columbia, Vancouver, BC V6T 1Z4, Canada.
B.D. Amiro[2] **and A.L. Orchansky.** Canadian Forest Service, Northern Forestry Centre, 5320 122 Street, Edmonton, AB T6H 3S5, Canada.
J.H. McCaughey. Department of Geography, Queen's University, Kingston, ON K7L 3N6, Canada.
L.B. Flanagan. Department of Biological Sciences, University of Lethbridge, 4401 University Drive, Lethbridge, AB T1K 3M4, Canada.
P.M. Lafleur. Department of Geography, Trent University, Peterborough, ON K9J 7B8, Canada.
N.T. Roulet. Department of Geography, McGill University, 805 Sherbrooke Street West, Montréal, QC H3A 2K6, Canada.
C.P.-A. Bourque. Faculty of Forestry and Environmental Management, University of New Brunswick, P.O. Box 44555, Fredericton, NB E3B 6C2, Canada.
M.A. Arain. School of Geography and Geology, McMaster University, 1280 Main Street West, Hamilton, ON L8S 4K1, Canada.
S.C. Wofsy and A. Dunn. Division of Engineering and Applied Science, Department of Earth and Planetary Science, Harvard University, 29 Oxford Street, Cambridge, MA 02138, USA.
P.Y. Bernier. Canadian Forest Service, Laurentian Forestry Centre, P.O. Box 3800, succursale Ste-Foy, Québec G1V 4C7, Canada.
J.M. Chen. Department of Geography and Program in Planning, University of Toronto, 100 George Street, Room 5047, Toronto, ON M5S 3G3, Canada.
N. Saigusa. National Institute of Advanced Industrial Science and Technology, Tsukuba West, Tsukuba 305-8569, Japan.
N. Hedstrom. National Water Research Institute, National Hydrology Centre, Environment Canada, 11 Innovation Boulevard, Saskatoon, SK S7N 3H5, Canada.

[1]Corresponding author (e-mail: Hank.Margolis@sbf.ulaval.ca).
[2]Present address: Department of Soil Science, University of Manitoba, Winnipeg, MB R3T 2N2, Canada.

 doi:10.1139/X05-270

forestiers, des peuplements résineux d'âge intermédiaire, des peuplements feuillus mûrs, des peuplements résineux mûrs, des tourbières arborées et une tourbière arbustive ouverte. Les variations diurnes de PNE étaient très cohérentes à l'intérieur des différentes catégories d'écosystème. Les stations récemment perturbées étaient associées au plus faible cycle diurne et les peuplements résineux d'âge intermédiaire étaient associés au plus fort cycle diurne. La tourbière arborée de l'ouest avait un patron diurne plus accentué que ceux de la tourbière arbustive de l'est et de la tourbière structurée de la Saskatchewan. Toutes les stations, sauf trois, constituaient clairement des puits de carbone en après-midi. Le plus fort taux de respiration de l'écosystème a été mesuré dans les stations récemment brûlées. Les plus fortes productivités maximales nette (PNE_{max}) et brute (PBE_{max}) de l'écosystème ont été mesurées dans les peuplements d'âge intermédiaire et ont atteint des taux qui seraient consistants avec la présence d'un fort puits terrestre de carbone dans les régions où ces types de forêt sont communs. Ces résultats supportent l'idée que les activités de modélisation du cycle du carbone à grande échelle bénéficieraient de l'information sur la distribution des classes d'âge et les types de perturbation à l'intérieur de cellules cartographiques plus grandes. L'efficacité d'utilisation de la lumière a suivi un patron semblable à celui des PNE_{max} et PBE_{max}. Quatre des cinq stations récemment perturbées et les trois stations couvertes par des tourbières ont montré de faibles valeurs d'efficacité d'utilisation de l'eau.

[Traduit par la Rédaction]

Introduction

Over the past 150 years, human activity has significantly altered the global carbon (C) cycle. This has been clearly manifested in the persistent and rapid rise in the level of greenhouse gases in the atmosphere (IPCC 2001). The two primary factors responsible for modifying the terrestrial C cycle are (*i*) extraction and emission of C from long-term stores of fossil fuels and (*ii*) changes in land cover and land use (Sarmiento and Gruber 2002). Increases in carbon dioxide (CO_2) and other greenhouse gases in the atmosphere have altered atmospheric C fluxes to both the oceans and the terrestrial biosphere (Battle et al. 2000; Bousquet et al. 2000; Rödenbeck et al. 2003). The potential importance of the biosphere to greenhouse warming is highlighted by the fact that annual fluxes from terrestrial ecosystems are more than an order of magnitude greater than fossil fuel emissions. Thus, it is important to understand the factors controlling the exchange of C between terrestrial ecosystems and the atmosphere, particularly at a continental scale. A major difficulty in determining the role of the biosphere in the global C cycle is the high degree of spatial heterogeneity in the sinks and sources and the extent to which humans have modified and continue to modify the landscape (Houghton 2003).

Eddy covariance (EC) flux towers permit the measurement of the turbulent fluxes of CO_2, water vapor, and energy between an ecosystem and the atmosphere. The measurements are typically obtained for spatial scales ranging from several hundred square metres up to a square kilometre (Schuepp et al. 1990) and are usually calculated for 30 min intervals (Baldocchi 1997, 2003). This methodology is the only means currently available for continuous, year-long, long-term measurements of ecosystem-level fluxes. Networks of such towers have been established in many of the major regions of the world, such as North America (Canada and the United States), Europe, Asia, and Oceania. These networks are a key component of global C cycle research and monitoring programs (Running et al. 1999; Global Carbon Project 2003).

The Fluxnet-Canada Research Network (FCRN) was established in 2002 to examine how management practices, natural disturbance, and climate variability influence C cycling in forest and peatland ecosystems in Canada. FCRN added a number of new flux sites to supplement those that had been previously installed so as to establish an east–west continental transect across the commercial forest zone of Canada (Fig. 1). The Canadian forest sector, including both forests and peatlands, covers more than 4×10^6 km^2 and accounts for more than 40% of the country's land surface (Kurz and Apps 1999). Several models have suggested that there has been a significant reduction in the C sink strength of Canadian forests since 1980 as a result of increased fire frequency (Kurz and Apps 1999; Chen et al. 2000). A major objective of FCRN is to provide the site-level process measurements and analyses needed to understand what might be expected as the age-class structure of Canadian forests changes over the coming decades under a potentially changing climate.

By late summer of 2003, flux measurements at most of our new sites had begun. The availability of an initial data set of 30 min net ecosystem productivity (NEP) measurements for 20 sites across the transect for August 2003 allowed us to examine some of the basic characteristics of the diurnal courses and maximum midday C sink or source strengths of forest and peatland ecosystems in Canada. The month of August is of interest because it includes the transition from mid- to late-summer conditions for many regions of Canada and is a period when significant water stress often occurs in the western portion of the country. In the current article, we compare average August diurnal courses of NEP for the mature, intermediate-aged, young, and recently disturbed stands being measured, as well as for a western minerotrophic treed fen, an eastern ombrotrophic shrub bog, and a southern patterned fen. We use light response curves to analyze maximum NEP (NEP_{max}), maximum gross ecosystem productivity (GEP_{max}), ecosystem respiration, light use efficiency, and water use efficiency (WUE) to determine if there is a general pattern with age since disturbance for the forest sites. We recognize that the transect data set is limited to 1 month during the growing season and that the effects of stand age can be confounded with phenological differences among sites across the transect and that this can have a significant impact on intersite comparisons of annual C accumulation. However, the advantage of assembling such a diverse data set is that it can test whether the strength of the signal coming from time since disturbance at a continental scale is strong enough to overcome all of the possible confounding effects.

Fig. 1. Location of Fluxnet-Canada flux measurement stations included in the current study.

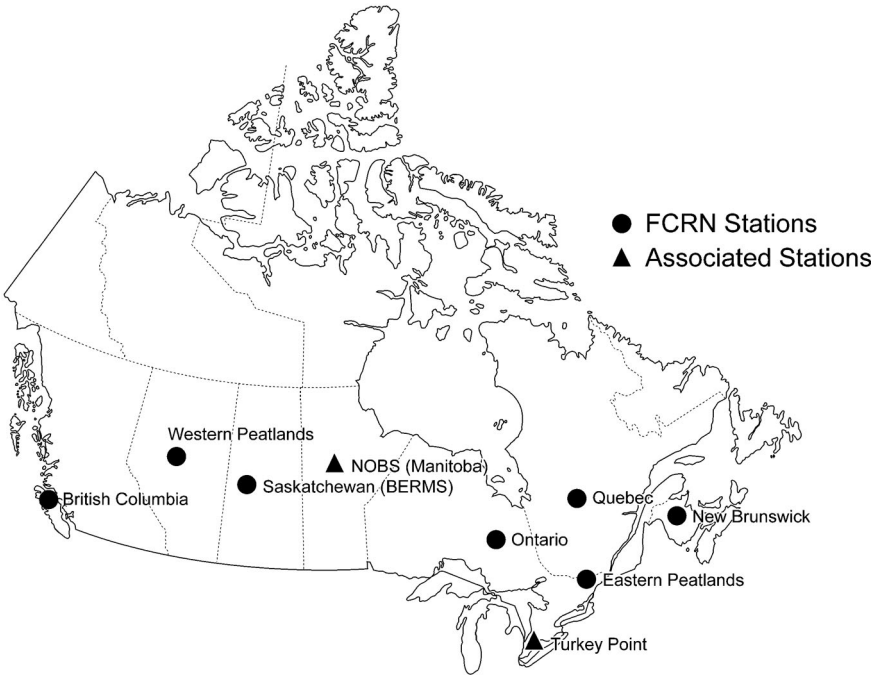

Materials and methods

Study sites

FCRN is composed of five main forest flux stations along a continental-wide transect stretching from Vancouver Island, British Columbia, to central New Brunswick in Canada (Tables 1 and 2, Fig. 1). Each forest flux station contains a cluster of flux towers having a minimum of one long-term tower in an undisturbed forest and one other tower that measures a forest disturbance scenario, such as harvest or fire (Tables 1 and 2). Two associated forest stations also participated in the current analysis (Fig. 1). The associated stations are externally funded, and although they are not obliged to follow all network measurement protocols, they contribute data for overall network analyses, such as that described here. FCRN has two peatland stations where a long-term tower is supplemented by a second tower that samples the spatial variability of fluxes among peatland ecosystems in a given region. Only the two long-term peatland towers at these stations are included in the present analysis. There is also a patterned fen that is part of the Saskatchewan (Boreal Ecosystem Research and Monitoring Sites program) Flux Station included in the present analysis.

The flux sites included in this study are described in Table 1. The sites fall into five of the seven major terrestrial ecozones in southern Canada (Pacific Maritime, Boreal Plains, Boreal Shield, Atlantic Maritime, and Mixedwood Plains) (NRCan 2003). The sites include five recently disturbed stands, three young stands, three intermediate-aged conifer stands, two mature deciduous stands, four mature conifer stands, and three peatland sites (Table 1). Canopy heights ranged from <0.1 to 33 m. Because the current analyses are an initial look at fluxes for a single month early in the life of our research network, we do not yet have data available for several key ecological variables, such as leaf area index and net primary productivity (NPP), for all sites. These data will be reported in subsequent manuscripts, as will the annual and multiannual fluxes.

Measurement standardization, data processing, and data archiving

Within the constraints of the existing equipment operating at the beginning of network activities, FCRN was designed to maximize standardization of (*i*) equipment; (*ii*) protocols for flux, meteorological, and ecological measurements; (*iii*) processing of high-frequency flux data; and when applicable, (*iii*) gap-filling algorithms for CO_2, heat, and water vapor fluxes. The basic configuration of the measurement systems for the different sites as they operated in August 2003 is described in Table 2.

The FCRN data information system provides a Web-based, easily accessible database that is available initially to network members and eventually to the scientific community at large (http://fluxnet.ccrp.ec.gc.ca). FCRN has also established a fair-use data policy (see Data policy section at http://www.Fluxnet-Canada.ca).

Flux measurements

The above-canopy CO_2 flux (F_c) and H_2O flux were measured near the top of each tower by using the EC method. Wind speeds were measured with a three-dimensional sonic anemometer, and CO_2 and H_2O concentrations were measured with either a closed-path or an open-path infrared gas analyzer (IRGA) (Table 2).

The net CO_2 and water vapor fluxes were obtained by calculating the mean covariance between the vertical wind speed and either the CO_2 or the H_2O mixing ratio for closed-path IRGAs or the CO_2 or H_2O density for open-path IRGAs for 30 min periods. When possible, CO_2 and H_2O high-frequency density fluxes were converted to mixing ratios before covariances were calculated. Otherwise, fluxes calculated us-

Table 1. Description of Fluxnet-Canada sites included in the present study.

Site	Code	Province	Location (°N,°W)	Terrestrial ecozone[a]	Ecoclimatic region[b]	Elevation (m a.s.l.)	Age[c] (years)	Stand origin[d]	Dominant species[e]	Canopy height (m)
Recently disturbed stands										
2002 harvested jack pine	HJP02	SK	53.945, 104.649	BP	SH, M–HB	580	1	H–P	JP	<0.1
2000 harvested black spruce	HBS00	QC	49.267, 74.037	BS	H, M–HB	392	3	H–P	KA, VA, BS	1.0
2000 harvested Douglas-fir	HDF00	BC	49.958, 125.433	PM	MPC	180	3	H–P	DF	0.5
1998 fire	F98	SK	53.917, 106.078	BP	SH, M–HB	540	5	F–N	JP, BS, TA	1.0–2.0
1994 harvested jack pine	HJP94	SK	53.908, 104.656	BP	SH, M–LB	580	9	H–P	JP	2.5
Young stands										
1988 Douglas-fir	DF88	BC	49.519, 124.902	PM	MPC	200	14	H–P	DF	5.5
1989 fire	F89	SK	54.254, 105.877	BP	SH, MB	520	14	F–N	JP, WB, TA, BP	5.0
1977 fire	F77	SK	54.485, 105.817	BP	SH, MB	590	26	F–N	JP, BS	7.4
Intermediate-aged stands										
Intermediate balsam fir	IBF	NB	46.472, 67.100	AM	T, HCT	340	35	H–N	BF	13.5
Intermediate Douglas-fir	IDF	BC	49.905, 125.366	PM	MPC	300	54	H–P	DF	33
White pine plantation	WPP	ON	42.712, 80.357	MP	H, MCT	184	60	A–P	WP	22
Mature deciduous stands										
Old mixedwood	OMW	ON	48.217, 82.156	BS	H, MB	341	74	F–PH–N	TA, WB, WS, BS, BF	21.6
Old aspen	OA	SK	53.629, 106.200	BP	SH, LB	601	84	F–N	TA	20.1
Mature conifer stands										
Old jack pine	OJP	SK	53.916, 104.690	BP	SH, LB	579	88	F–N	JP	15.6
Eastern old black spruce	EOBS	QC	49.692, 74.342	BS	H, M–HB	393	100	F–N	BS, JP	14.0
Southern old black spruce	SOBS	SK	53.987, 105.117	BP	SH, M–LB	629	123	F–N	BS	11
Northern old black spruce	NOBS	MN	55.880, 98.481	BS	SH, HB	259	167	F–N	BS	9.1
Peatlands										
Western peatland	WP	AB	54.954, 112.465	BP	SH, LB	577	na	na	TM, BS	2.9
Southern fen	SFEN	SK	53.481, 105.366	BP	SH, M–LB	486	na	na	CA, BB, TM	0.5
Eastern peatland	EP	ON	45.409, 75.520	MP	H, HCT	70	na	na	CH, KA, LG	0.3

Note: na, not applicable.

[a]Ecozones (NRCan 2003): AM, Atlantic Maritime; BP, Boreal Plains; BS, Boreal Shield; MP, Mixedwood Plains; PM, Pacific Maritime.

[b]Ecoregions (Ecoregions Working Group 1989): H, humid; HB, high boreal; HCT, high cool temperate; LB, low boreal; MB, mid boreal; MCT, mid cool temperate; M–HB, mid–high boreal; M–LB, mid–low boreal; MPC, maritime Pacific Cordilleran; SH, subhumid; T, transitional.

[c]Age since disturbance.

[d]A, abandoned agricultural land; F, fire; H, harvested; N, natural regeneration; P, planted; PH, partially harvested (high grading).

[e]Dominant species: BB, bog birch (*Betula glandulosa* Michx.); BF, balsam fir (*Abies balsamea* (L.) Mill.); BP, balsam poplar (*Populus balsamifera* L.); BS, black spruce (*Picea mariana* (Mill.) BSP); CA, *Carex* spp.; CH, *Chamaedaphne calyculata* (L.) Moench); DF, Douglas-fir (*Pseudotsuga menziesii* (Mirb.) Franco); JP, jack pine (*Pinus banksiana* Lamb.); KA, *Kalmia angustifolia* L.; LG, *Ledum groenlandicum* Oeder; TA, trembling aspen (*Populus tremuloides* Michx.); TM, tamarack (*Larix laricina* (Du Roi) K. Koch); VA, *Vaccinium angustifolium* Ait.; WB, white birch (*Betula papyrifera* Marsh.); WP, white pine (*Pinus strobus* L.); WS, white spruce (*Picea glauca* (Moench) Voss).

Table 2. Measurement and related systems operating in August 2003.

Site code	Measurement height[a] (m)	Sonic anemometer[b]	Flux IRGA[c]	Sampling frequency (Hz)	Threshold u_* ($m \cdot s^{-1}$)	Days of flux data	Power source
Recently disturbed stands							
HJP02	3	CSAT3	LI-7500	20	0.15	31	Line
HBS00	7	CSAT3	LI-7500	10	0.15	31	Solar
HDF00	3	Gill R3	LI-6262	20	0.10	31	Propane, solar
F98	20	CSAT3	LI-7500	10	0.25	31	Solar
HJP94	5	SAT-550	LI-6262	10	0.10	31	Line
Young stands							
DF88	12	Gill R3	LI-7000	20	0.15	31	Propane, solar
F89	10	CSAT3	LI-7500	10	0.25	31	Solar
F77	12	CSAT3	LI-7500	10	0.30	31	Solar
Intermediate-aged stands							
IBF	20	CSAT3	LI-7500	10	0.20	19	Solar, wind
IDF	43	Gill R2	LI-6262	20.83	0.30	31	Diesel
WPP	28	CSAT3	LI-7000	20	0.25	31	Line
Mature deciduous stands							
OMW	41	CSAT3	LI-7500	10	0.20	22	Line
OA	39	Gill R3	LI-6262	20.83	0.30	31	Line
Mature coniferous stands							
OJP	28	CSAT3	LI-6262	10	0.30	31	Line
EOBS	25	CSAT3	LI-7500	10	0.20	31	Line
SOBS	25	Gill R3	LI-6262	20.83	0.30	31	Line
NOBS	30	ATI/3K	LI-6262	4	0.20	31	Diesel
Peatland sites							
WP	9	CSAT3	LI-7500	10	0.25	31	Line
SFEN	2.5	CSAT3	LI-7500	20	0.10	31	Line
EP	3	Gill R3	LI-6262	10	0.10	31	Line

[a]Height of eddy covariance flux measurement system.
[b]CSAT3: Campbell Scientific, Logan, Utah, USA; Gill R2, Gill R3: Gill Instruments Ltd., Lymington, Hampshire, UK; SAT-550: Kaijo Sonic Co., Japan; ATI/3K: Applied Technologies Inc., Longmont, Colorado, USA.
[c]LI-6262 (closed path), LI-7000 (closed path), LI-7500 (open path): LI-COR Inc., Lincoln, Nebraska, USA.

ing CO_2 and H_2O densities were corrected for heat and water vapor fluctuations (Webb et al. 1980). For the main network sites, the closed-path IRGAs (LI-6262 or LI-7000) were enclosed in a temperature-controlled housing (TCH), permitting year-round operation. Air sampled within 30 cm of the sonic array was drawn down a heated tube 4 m long and through the IRGA at 10–20 $L \cdot min^{-1}$. Open-path IRGAs were mounted within 30 cm of the sonic array. The wind vectors and associated covariances were mathematically rotated following the method described by Tanner and Thurtell (1969).

In this article, net C flux is presented as NEP in μmol $CO_2 \cdot m^{-2} \cdot s^{-1}$. The values for NEP are equal to the negative value of net ecosystem exchange (NEE) if losses of dissolved C are a negligible component of the overall budget at the time scale of the measurement, a reasonable assumption for our forest sites in August, but perhaps less so for our peatlands. The value for NEP is positive when the land surface is a C sink, whereas the value for NEE is positive when the land surface is a C source. We calculated NEE as $F_c + \Delta S/\Delta t$, where F_c is the above-canopy flux; and $\Delta S/\Delta t$ is the CO_2 storage flux in the air column beneath the EC sensors, calculated as the difference between the subsequent and the previous half-hour periods (Baldocchi et al. 1997). Values for CO_2 storage fluxes were calculated for all intermediate-aged stands and mature forested sites where data were available and for all fire sites, as well as for peatland sites WP and EP. With the exception of site EOBS, CO_2 storage fluxes were calculated using above-canopy CO_2 measurements made by the EC system. The CO_2 storage flux for site EOBS was calculated using integrated storage fluxes from a five-level CO_2 profile measurement system. There were no storage data available for sites OMW and IBF. Storage fluxes were not calculated for the recently harvested sites or for site SFEN because of the short stature and sparse cover of the vegetation on these sites (see Table 1), the influence of CO_2 storage on the net flux being negligible for open and for shorter canopies. Site OMW was missing approximately 9 days of flux during the month, and site IBF did not have fluxes for the first 10 days of the month (see Table 2).

Air temperature and photosynthetically active radiation flux

Air temperature and photosynthetically active radiation (PAR) flux (Q_i) were measured at the height of the flux measurements. Monthly averages, including average diurnal courses, were calculated. Measurements of Q_i were taken either by an LI-189

or LI-190 quantum sensor (LI-COR Inc., Lincoln, Nebraska) or by a BF-2 or BF-3 sunshine sensor (Delta-T Instruments, Cambridge, UK).

Diurnal courses of NEP

Nighttime data ($Q_i < 5$ μmol·m^{-2}·s^{-1}) with low friction velocities (u_*) were removed so that unbiased estimates of NEP could be obtained (Goulden et al. 1996). The u_* thresholds were site specific and ranged from 0.1 to 0.3 m·s^{-1} (Table 2). Data points left after the removal of low friction velocities covered a wide range of dates in the month of August, and there were no long, continuous gaps. The average diurnal course of NEP for the month of August was calculated using each half-hour period, providing a total of 48 points for the month. Data were not gap-filled, as this procedure requires a longer time series than was available for this initial analysis.

Light response curves to derive maximum NEP and GEP

Light response curves were fit to NEP data when Q_i was >0 μmol·m^{-2}·s^{-1} and u_* exceeded threshold site friction velocity. Outliers were removed when they were greater than three standard deviations from the mean at a given level of PAR. Outliers involved <1% of the data points. The Landsberg equation (Landsberg 1977; Chen et al. 2002*a*) was used for fitting the light response curves:

$$[1] \quad \mathrm{NEP} = \mathrm{NEP}_{max}\{1 - \exp[-\alpha(Q_i - \Gamma)]\}$$

where NEP_{max} is the asymptote of the light response curve; α is the quantum efficiency parameter (mol CO_2·(mol PAR)$^{-1}$); Q_i is the incident photosynthetic photon flux density (μmol PAR·m^{-2}·s^{-1}); and Γ is the light compensation point (μmol PAR·m^{-2}·s^{-1}). Estimates of NEP_{max}, α, and Γ were derived for individual sites, with the exception of site HJP02, and for combinations of sites (ecosystem age categories) by using nonlinear regression with MATLAB 6.5 (MathWorks Inc., Natick, Massachusetts). This procedure also calculates the 95% confidence intervals for the parameter estimates. In this article, we examine primarily the NEP_{max} parameter.

As described in Griffis et al. (2003), the average total ecosystem respiration (R_{eco}) for the month was estimated from the *y* intercept of the light response curve that had been fit for each site; that is, $R_{eco} = \mathrm{NEP}_{max}\{1 - \exp[-\alpha(0 - \Gamma)]\}$. This R_{eco} value represents the respiration for the average daytime temperature conditions present on a given site. Griffis et al. (2003) showed that conducting the calculation for different ranges of air temperature had only a small effect on the estimate. The time series of data for many of our sites was too limited to permit a calculation of daytime respiration from the temperature versus nighttime flux relationship that is often used in longer term studies (Falge et al. 2001).

The NEP–Q_i relationship described by the Landsberg equation did not hold for site HJP02 data, as the NEP values rarely surpassed zero at high-Q_i conditions. Consequently, NEP_{max} and R_{eco} for site HJP02 were estimated by calculating the mean C flux where PAR is greater than 1500 and less than 25 μmol·m^{-2}·s^{-1}, respectively.

The GEP_{max} for the month was calculated from R_{eco} and NEP_{max}:

$$[2] \quad \mathrm{GEP}_{max} = R_{eco} + \mathrm{NEP}_{max}$$

Light use efficiency

The average light use efficiency (ε) for the month of August, with respect to incident PAR flux, was calculated as follows:

$$[3] \quad \varepsilon = \frac{\mathrm{GEP}_{day}}{Q_{day}}$$

where Q_{day} (mol·m^{-2}·day^{-1}) is the mean total daytime Q_i for August, which was calculated from the mean diurnal pattern of Q_i (mol PAR·m^{-2}·s^{-1}) by summing the 30 min integrations of Q_i over periods when the mean 30 min Q_i was >5 μmol·m^{-2}·s^{-1}; and GEP_{day} (mol CO_2·m^{-2}·day^{-1}) is the daily gross ecosystem productivity, calculated as follows:

$$[4] \quad \mathrm{GEP}_{day} = \sum \mathrm{NEP} + R_{day}$$

where $\sum$NEP (mol·m^{-2}·day^{-1}) is the mean total daytime NEP for August, which was calculated from the mean diurnal pattern of NEP (mol·m^{-2}·s^{-1}) by summing the 30 min integrations of NEP over periods when the mean 30 min Q_i was >5 μmol·m^{-2}·s^{-1}. Similarly, R_{day} (mol·m^{-2}·day^{-1}) was calculated by multiplying R_{eco} (μmol·m^{-2}·s^{-1}) by the average number of seconds during the day when the 30 min mean Q_i was >5 μmol·m^{-2}·s^{-1}.

Water use efficiency index, daytime water flux, and evaporative fraction

An index of ecosystem WUE (g CO_2·(kg H_2O)$^{-1}$) was calculated as

$$[5] \quad \mathrm{WUE} = \frac{\mathrm{GEP}_{day}}{E_{day}}$$

where E_{day} (kg H_2O·m^{-2}·day^{-1}) is the mean total daytime H_2O flux for August calculated from the mean diurnal pattern of H_2O flux (g H_2O·m^{-2}·s^{-1}) by summing the 30 min integrations of the H_2O flux over periods when the mean 30 min Q_i was >5 μmol·m^{-2}·s^{-1}; and GEP_{day} is expressed in g CO_2·m^{-2}·day^{-1}.

The evaporative fraction (EF) was calculated as follows:

$$[6] \quad \mathrm{EF} = \frac{\mathrm{LE}_{day}}{R_{n\text{-}day}}$$

where LE_{day} is the mean total water (latent energy) flux, that is, E_{day}, when expressed in J·m^{-2}·day^{-1}; $R_{n\text{-}day}$ (J·m^{-2}·day^{-1}) is the mean total daytime net radiation for August, which was calculated from the mean diurnal pattern of net radiation (J·m^{-2}·s^{-1}) by summing the 30 min integrations of net radiation over periods when the mean 30 min Q_i was >5 μmol·m^{-2}·s^{-1}. EF was not calculated for HJP02 and SFEN because $R_{n\text{-}day}$ was not available.

Results

Air temperature and PAR flux

Air temperature varied between regions across the transect. Mean daily maximum temperature ranged from 26.5 °C at site SFEN in Saskatchewan to 20.9 °C at site OMW in

Ontario (Table 3). Similarly, mean daily minimum temperatures ranged from 16.2 °C at site WPP in Ontario to 7.8 °C at site WP in Alberta. Mean daily maximum Q_i ranged from 933 μmol·m^{-2}·s^{-1} at site WPP to 507 μmol·m^{-2}·s^{-1} at site HBS00 in Quebec (Table 3).

Diurnal cycles of NEP

The average diurnal courses of NEP for August 2003 showed strong coherence within each of the six categories of ecosystems (Fig. 2). All the recently disturbed (≤9 years) forest ecosystems, as well as the open shrub bog (site EP) and the patterned fen (site SFEN), showed, at most, only weak diurnal cycles (Figs. 2*a* and 2*f*). The recently disturbed black spruce site (HBS00) and the recent fire site (F98) were small afternoon sinks, whereas the other recently disturbed sites were either C neutral or sources of C in the afternoon (Fig. 2*a*). Site HDF00, in British Columbia, showed a more negative NEP between midnight and early morning than the other recently disturbed sites (Fig. 2*a*).

The diurnal cycle for the young conifer stands (14–26 years old) (Fig. 2*b*) was more pronounced and was similar to that observed for the two mature deciduous sites (74–84 years old) (Fig. 2*d*). The intermediate-aged conifer stands (35–60 years old) had the most pronounced diurnal cycle (Fig. 2*c*). Site IBF in New Brunswick was a greater sink for CO_2 during the afternoon than sites IDF and WPP in British Columbia and southern Ontario, respectively (Fig. 2*c*). The four mature conifer stands (88–167 years old) (Fig. 2*e*) had NEP values similar to the treed fen (site WP) in Alberta (Fig. 2*f*). Site WP had a more pronounced diurnal pattern than either the open shrub bog (site EP) or the patterned fen (site SFEN) (Fig. 2*f*).

Maximum NEP, maximum GEP, and ecosystem respiration

The values of NEP_{max}, GEP_{max}, and R_{eco} derived from fitting site-level light response curves (Table 4) showed clear patterns with respect to age since disturbance (or age since planting in the case of site WPP) (Fig. 3). The intermediate-aged conifer and mature deciduous stands generally had the highest NEP_{max} and GEP_{max} values (Figs. 3*a* and 3*b*), with site IBF in New Brunswick showing the strongest maximum sink. The two older fire sites (F89 and F77) had high GEP_{max} values, although their NEP_{max} values were generally closer to those of the recently disturbed sites. The four recently harvested stands (sites HJP02, HBS00, HDF00, and HJP94) had the lowest GEP_{max} and NEP_{max}.

Values of R_{eco} (Fig. 3*c*) generally followed the same pattern with age as NEP_{max} and GEP_{max}, except that sites F77 and F89 had the highest R_{eco} and intermediate-aged conifer site IBF had a lower R_{eco} than intermediate-aged conifer sites IDF and WPP (Fig. 3*c*).

The treed fen (site WP) in Alberta had GEP_{max}, NEP_{max}, and R_{eco} values similar to those of the mature conifer stands, whereas the values for the shrub bog (site EP) in Ontario and for the patterned fen (site SFEN) in Saskatchewan were similar to those for the recently disturbed stands. Among the three peatland sites, the NEP_{max}, GEP_{max}, and R_{eco} values were higher for site WP than for site EP or site SFEN (Fig. 3).

Light response functions for ecosystem categories

Light response curves fit to each of the six ecosystem categories showed that NEP_{max} was highest for the intermediate-aged conifer stands (16.3 μmol·m^{-2}·s^{-1}) and mature deciduous stands (10.2 μmol·m^{-2}·s^{-1}) and lowest for the young and recently disturbed sites (Fig. 4). The goodness of fit for these light response curves was also greatly affected by age since disturbance and by ecosystem type. Curves fit to data from recently disturbed sites, young stands, and peatland sites had lower R^2 values (0.27, 0.40, and 0.35, respectively), whereas those fit to data from the other ecosystem types had R^2 values of 0.54 or higher.

Light use efficiency

Light use efficiencies (ε) based on incident PAR (Fig. 5*a*) for each forested and peatland site showed the same general pattern as those for NEP_{max} and GEP_{max}, an increase up to around 60 years after disturbance, followed by a decrease. However, ε values for the two Quebec sites (HBS00 and EOBS), where Q_i levels were low in August, were higher than for the other sites in their respective ecosystem category. This was not the case for NEP_{max} or GEP_{max}.

Water use efficiency index, daytime water flux, and evaporative fraction

Intermediate-aged conifer site IDF in British Columbia had by far the highest WUE (24.2 g CO_2·kg^{-1} H_2O) of any of the sites, and recently harvested site HJP02 in Saskatchewan had the lowest (0.2 g·kg^{-1}, Fig. 5*b*). Of the recently disturbed sites, HDF00 had the highest WUE, at 12.9 g·kg^{-1}; HJP02 had the lowest; and the other three sites had intermediate values ranging from 4.3 to 6.6 g·kg^{-1}. The WUE values for the young stands ranged from 9.0 to 14.4 g·kg^{-1} and were similar to those for intermediate-aged conifer sites IBF and WPP. The mature deciduous and conifer stands had WUEs that ranged from 4.6 to 10.5 g·kg^{-1}, site OA having the lowest and site OMW the highest (Fig. 5*b*). Of the peatland sites, WP had a WUE approximately twice as high as the WUEs of the other two peatland sites.

Values for water flux (E_{day}) and the evaporative fraction (EF) followed the same pattern (Fig. 6). With the exception of site F98, the recently disturbed sites in the western part of Canada had relatively low E_{day} and EF values within their respective ecosystem categories; the recently disturbed site in eastern Canada (HBS00) had relatively high values (Fig. 6). As well, all three Douglas-fir sites in British Columbia (HDF00, DF88, IDF) had low E_{day} and EF values. The fire sites, intermediate-aged conifer sites IBF and WPP, and mature mixedwood site OMW had the highest E_{day} and EF values, and these values were similar to those for the peatland sites.

Discussion

Importance of seral stage

The relative consistency of the mean August diurnal courses of NEP for August 2003 within each of the ecosystem categories and the degree to which the apparent variability in fluxes was associated with age since disturbance are two striking results from the current analysis (see

Table 3. Mean daily air temperature, mean daily maximum and minimum air temperatures, mean daily total photosynthetic photon flux density, mean daily maximum photosynthetic photon flux density, and rainfall for all sites for the month of August.

	Mean air temperature (°C)					August precipitation (mm)	
Site code	Daily	Max.	Min.	Q_{day} (mol·m^{-2}·day^{-1})[a]	Mean max. Q_i (μmol·m^{-2}·s^{-1})[b]	2003[c]	Historic[d]
Recently disturbed stands							
HJP02	18.2	26.2	9.9	11 708	820	48	60
HBS00	16.2	21.4	11.9	6 871	507	143	105
HDF00	17.6	24.5	10.6	11 205	797	6	49
F98	17.9	26.3	10.3	11 546	805	43	60
HJP94	18.9	26.4	11.8	12 048	834	17	60
Young stands							
DF88	17.6	23.0	12.4	12 111	868	1	35
F89	16.8	26.2	8.6	11 081	791	59	58
F77	16.2	24.9	8.2	11 427	847	58	58
Intermediate-aged stands							
IBF	16.9	22.2	12.7	8 833	814	99	108
IDF	16.8	21.7	13.1	11 370	807	41	49
WPP	20.5	25.0	16.2	12 436	933	41	81
Mature deciduous stands							
OMW	17.9	20.9	14.8	10 148	796	88	82
OA	19.2	25.4	14.2	11 436	792	61	60
Mature coniferous stands							
OJP	19.1	25.6	13.3	10 940	766	25	60
EOBS	16.1	21.1	11.7	7 260	570	143	105
SOBS	19.6	25.9	14.4	11 311	794	23	58
NOBS	18.9	24.9	13.9	9 764	748	57	74
Peatlands							
WP	15.6	23.6	7.8	10 886	777	18	63
SFEN	18.4	26.5	10.2	11 131	777	40	58
EP	19.9	26.3	13.7	10 075	814	42	95

[a]Daily integrated flux of incident photosynthetically active radiation measured at each site for August 2003.
[b]Mean daily maximum flux of incident photosynthetically active radiation measured at each site for August 2003.
[c]Total precipitation measured at each site or at the closest weather station for August 2003.
[d]Historic 30-year mean total precipitation measured at the closest weather station for the month of August.

Figs. 2 and 3). These results provide additional evidence of the importance of seral stage and disturbance history on C cycling dynamics in Canada at a continental scale. The national C budget of the Canadian forest sector is strongly influenced by disturbance regimes that are dominated by wildfire, insect infestations, and forest harvest. A modeling analysis based on historical inventory data by Kurz and Apps (1999) concluded that age-class structure controlled the C dynamics in the Canadian forest sector from 1920 to 1979, resulting in increased C sequestration. Subsequently (1980–1989), C sequestration decreased as a result of increased fire and insect disturbance and decreased average age. A similar analysis by Chen et al. (2000) also highlighted the importance of disturbance history, although they pointed out that an inventory-based analysis assumes constant growth and yield relationships over the period of the analysis.

Our data show that midsummer GEP_{max} and NEP_{max} scale to each other across the range of sites and ages such that the general patterns for both variables with age since disturbance are similar (Fig. 3). Although species composition, location, and climate for our sites varied along the transect, the results do suggest a general pattern with age. The NPP and NEP measured at boreal forest sites have been reported as increasing (from a net source) until stands reached an age of about 20–120 years and then slowly decreasing thereafter (Wirth et al. 2002; Litvak et al. 2003; Bond-Lamberty et al. 2004; Howard et al. 2004; Pregitzer and Euskirchen 2004; Martin et al. 2005). The rates of increase in these variables over the initial decades likely reflect a combination of the rates of crown closure, the rates of decomposition of the organic legacy left by the disturbance, and changes in species composition.

It is important to note that the current transect data represent only a single month during the growing season and that differences in phenology between sites along the transect could result in large differences in annual C accumulation or loss among sites, irrespective of the stage of successional development. In the present paper, we have concentrated on data for August and on parameters that can be readily calcu-

Fig. 2. August 2003 diurnal courses of net ecosystem productivity (NEP) for (*a*) recently disturbed stands (1–9 years old); (*b*) young stands (14–26 years old); (*c*) intermediate-aged conifer stands (35–60 years old); (*d*) mature deciduous stands (74–84 years old); (*e*) mature conifer stands (88–167 years old); and (*f*) peatland sites.

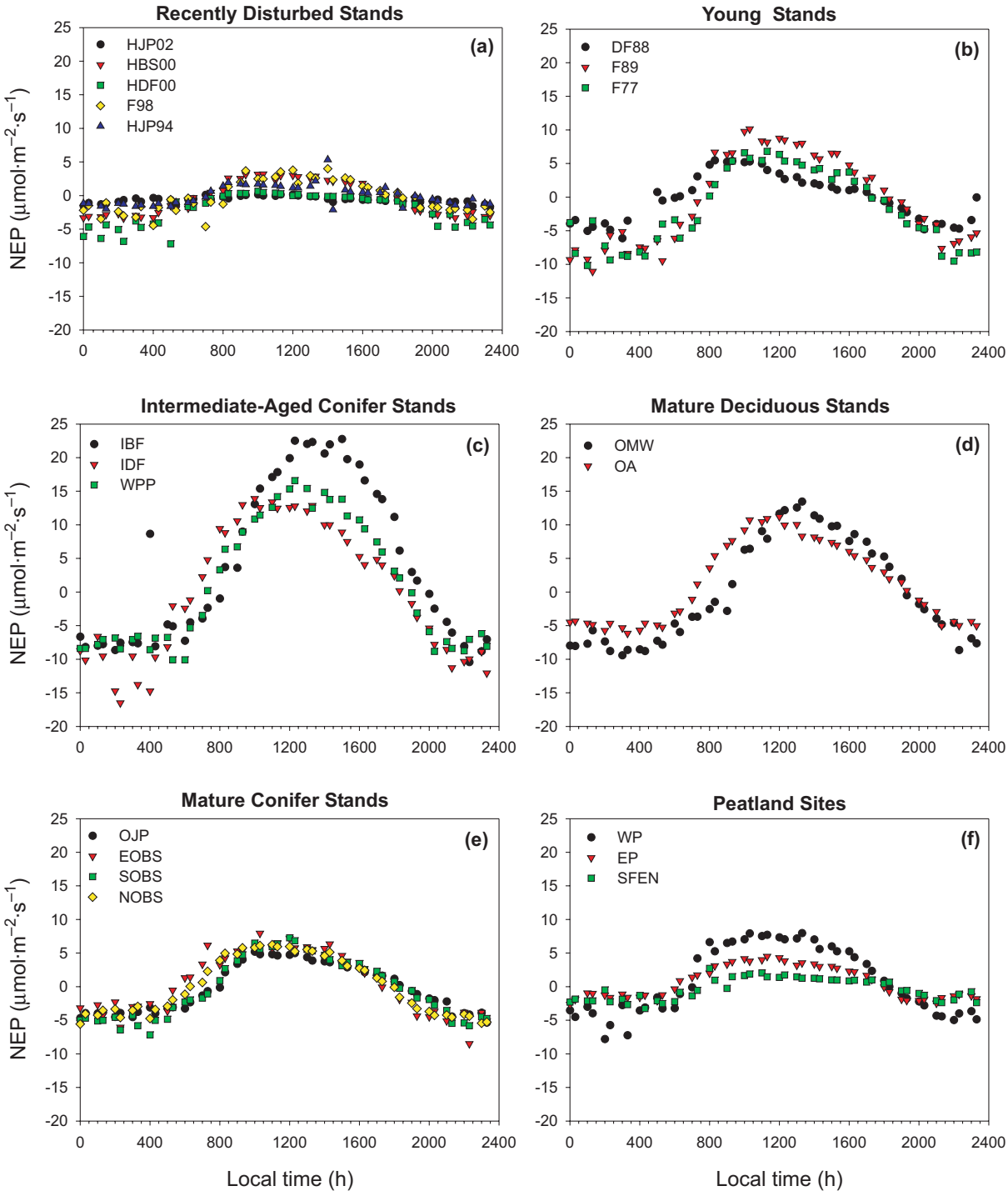

lated from a single month of flux data. Our more continuous gap-filled data sets for Saskatchewan show that August is a period when both young stands (sites F98, F89, HJP94) and mature conifer forests (sites OJP, SOBS) can have negative NEP values for the full month (Amiro et al. 2006). In contrast, the mature deciduous stand (site OA) remains a C sink throughout the summer. At one intermediate-aged stand (site IDF), depending on the year, August can be either a net source or a sink (Morgenstern et al. 2004). In southern Ontario, positive NEP values were observed at another intermediate-aged stand (site WPP) for every month from April to October (Arain and Restrepo-Coupe 2005). Hence, our conclusions for ecosystem fluxes in late summer of 2003 do not necessarily apply for full annual cycles, for earlier or

Table 4. Parameters estimated for the light response function, $NEP = NEP_{max}\{1 - \exp[-\alpha(Q_i - \Gamma)]\}$, fit to NEP and photosynthetic photon flux density data from individual Fluxnet-Canada sites.

Site code	NEP_{max} (μmol $CO_2 \cdot m^{-2} \cdot s^{-1}$)[a]	α (mol CO_2 (mol PAR)$^{-1}$)	Γ (μmol PAR$\cdot m^{-2} \cdot s^{-1}$)	R^2
Recently disturbed stands				
HJP02[b]	–0.36±1.15	—	—	—
HBS00	2.42±0.24	0.007 669	108.7	0.54
HDF00	0.02±0.11	0.007 002	730.6	0.38
F98	3.86±0.78	0.001 700	323.9	0.44
HJP94	1.41±0.20	0.004 554	152.6	0.47
Young stands				
DF88	3.00±0.29	0.005 963	164.7	0.21
F89	8.24±0.7	0.002 963	248.5	0.51
F77	6.02±0.70	0.002 467	376.3	0.55
Intermediate-aged stands				
IBF	23.29±1.93	0.001 461	118.8	0.71
IDF	11.71±0.75	0.003 559	146.0	0.51
WPP	17.37±1.45	0.001 280	198.4	0.60
Mature deciduous stands				
OMW	11.90±0.99	0.002 393	195.4	0.73
OA	9.38±1.13	0.003 193	138.0	0.64
Mature coniferous stands				
OJP	4.39±0.43	0.003 124	190.9	0.48
EOBS	6.36±0.57	0.003 866	118.9	0.63
SOBS	5.98±0.53	0.002 440	232.8	0.54
NOBS	5.22±0.35	0.003 845	161.7	0.55
Peatlands				
WP	8.76±0.74	0.001 895	193.6	0.67
SFEN	1.44±0.15	0.004 223	207.0	0.42
EP	3.76±0.21	0.004 157	93.1	0.46

[a] NEP_{max} ± 95% confidence interval.
[b] NEP_{max} ± 1 SD for site HJP02 was calculated as the mean of all NEP values corresponding to $Q_i >$ 1500 μmol$\cdot m^{-2} \cdot s^{-1}$.

later times in the growing season, or for other years. Furthermore, 2003 was a year of significant drought in western Canada (Barr et al. 2004; Hogg et al. 2005).

Fan et al. (1998) used atmospheric inversion to estimate a North American terrestrial C sink of 1.7 ± 0.5 Pg C$\cdot$year^{-1} for 1988–1992 that was largely located in eastern North America, south of latitude 51°N. Other studies have subsequently estimated a smaller North American sink, but they all still suggest that the eastern portion of the continent is an active C sink (Pacala et al. 2001; Gurney et al. 2002). A strong C sink in eastern North America is consistent with the high midsummer NEP rates that we measured for our intermediate-aged forests in eastern Canada. The annual C balance for the sites on our transect will shed more light on this issue.

The similarity in the patterns of the light response functions for a given ecosystem type (see Fig. 4) reinforces the idea that understanding and quantifying the disturbance history at local, regional, and continental scales is key to quantifying the terrestrial C budget and its sensitivity to climate change (e.g., Foster and Aber 2004; Wofsy 2004). At regional and continental scales, remote sensing techniques could play a major role in furthering our understanding. Recent increases in computing power and the capacity for large-scale processing of Landsat data offer the near-term potential for continental-level disturbance mapping (Masek et al. 2001; Cihlar et al. 2003; Cohen and Goward 2004). This approach needs to be integrated with forest inventory analysis to account for disturbance at longer time scales. Given the apparently important role of age since disturbance on the midsummer sink strength of forest ecosystems in Canada, we suggest that large-scale C cycle modeling activities would benefit significantly from information on the fractional age-class distributions within larger grid cells (see also Litvak et al. 2003).

Carbon flux and NPP

The NEP over a given period is the relatively small difference between the gain of C by an ecosystem through NPP and the loss through heterotrophic respiration and disturbance (Chen et al. 2000). Chen et al. (2002*b*), Bond-Lamberty et al. (2004), Howard et al. (2004), and Martin et al. (2005) reported NPP versus age relationships for black spruce, jack pine, and mixedwood chronosequences in Canada that were similar to the relationship we found between age and both

Fig. 3. August 2003 values of (*a*) NEP_{max}, (*b*) GEP_{max}, and (*c*) R_{eco} calculated for individual forest sites versus age since disturbance (or planting) and for peatland sites (far right). Values were obtained from fitting individual site-level light response curves (see eq. 1).

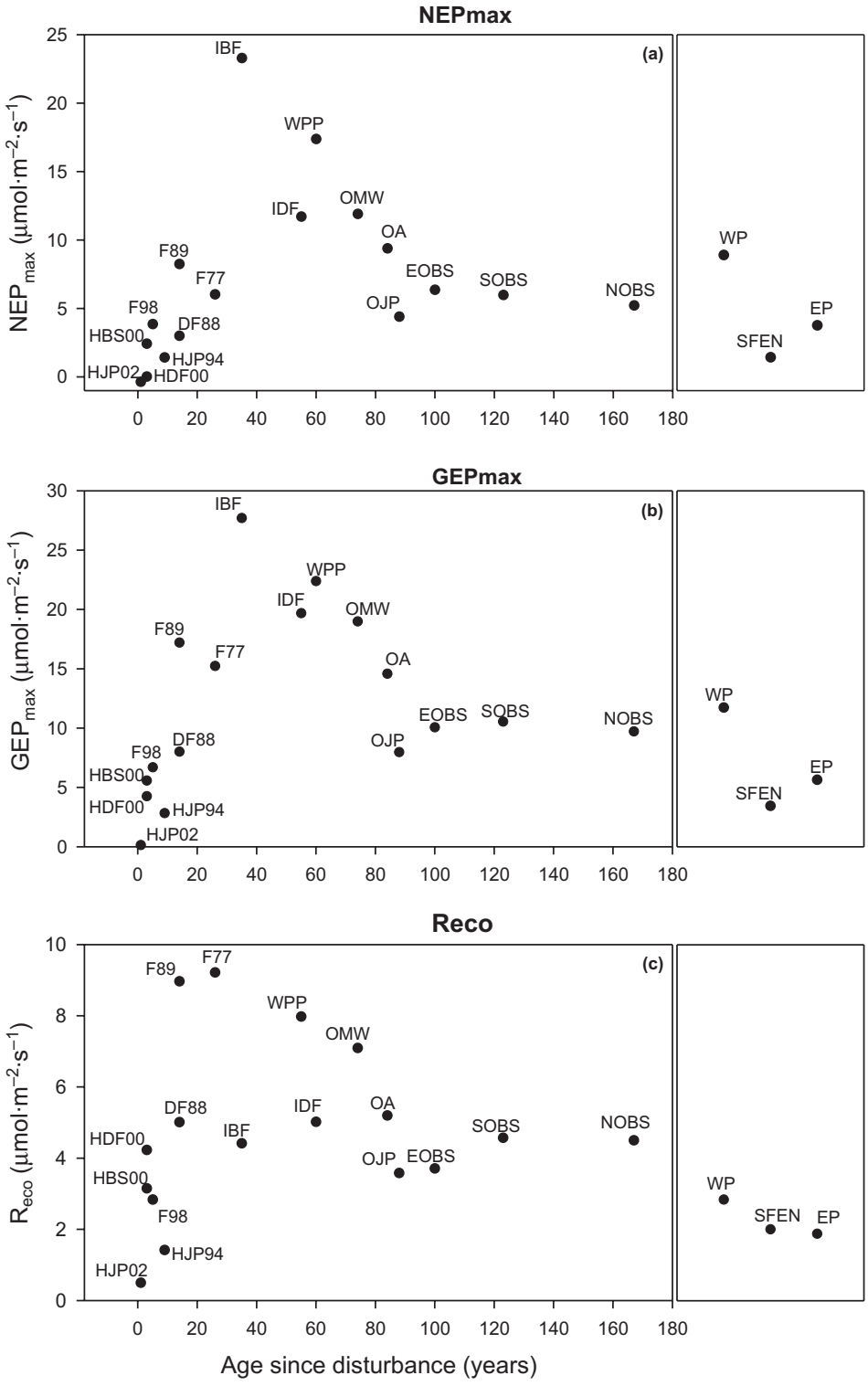

NEP_{max} and GEP_{max} in the current study. This supports the idea that the successional states having the highest productivity also have higher short-term rates of C sequestration, although we caution that the fluxes that we report here are only for a single month. Thompson et al. (1996) concluded that the long-term maintenance of a terrestrial C sink requires that NPP continue to increase so that heterotrophic respiration is never able to equilibrate with the increased litterfall resulting from the initial increase in NPP. A land area with significant amounts of intermediate-aged forest should exhibit such a

Fig. 4. August 2003 values of net ecosystem productivity (NEP) versus Q_i and the best fit of the Landsberg equation, NEP = $NEP_{max}\{1 - \exp[-\alpha(Q_i - \Gamma)]\}$, for (*a*) recently disturbed stands; (*b*) young stands; (*c*) intermediate-aged conifer stands; (*d*) mature deciduous stands; (*e*) mature conifer stands; and (*f*) peatland sites (NEP_{max} ± confidence interval).

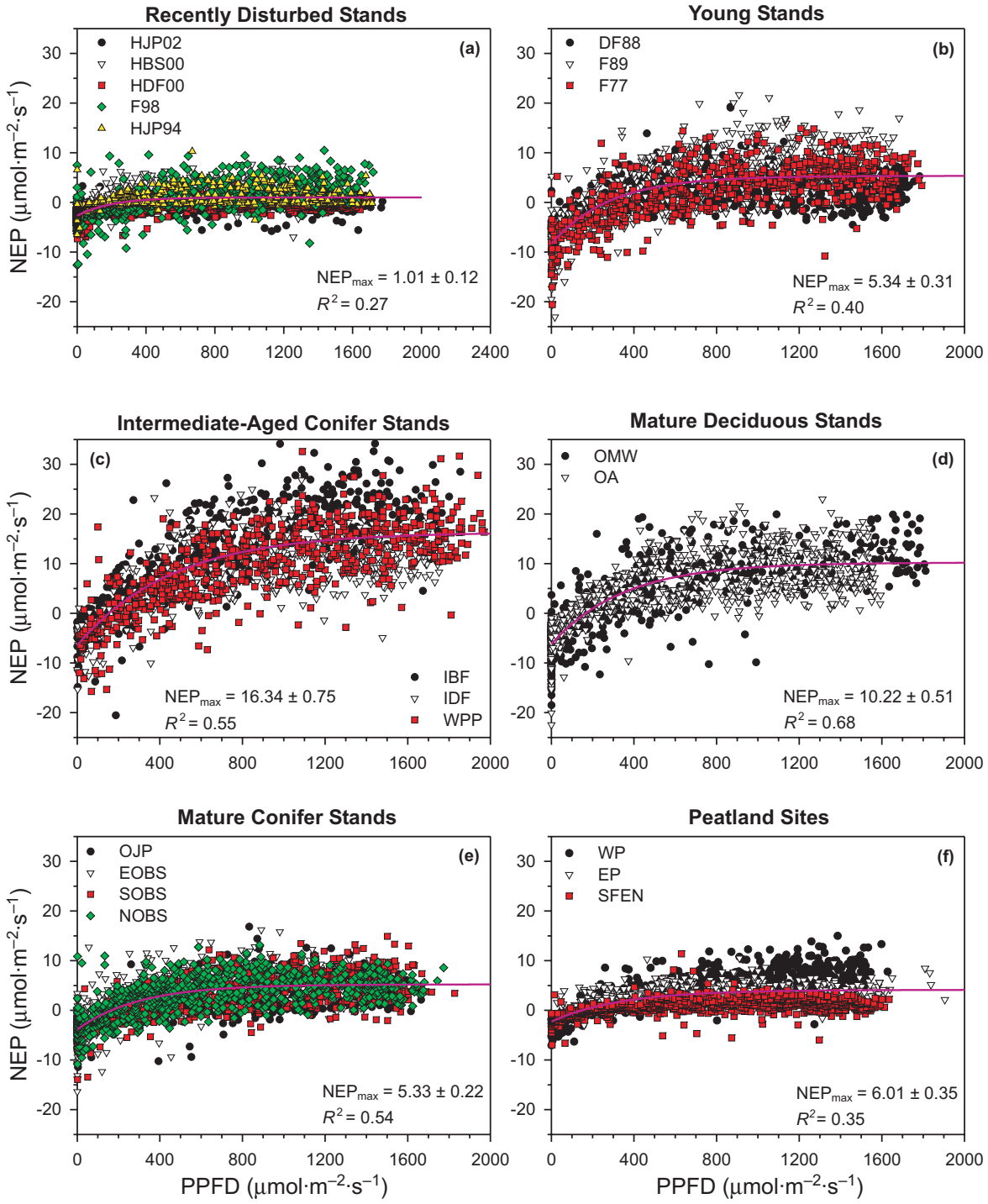

positive rate of increase in NPP and NEP over a period of several decades.

The apparent decreases in late-summer GEP_{max}, R_{eco}, and NEP_{max} values measured in mature stands compared to those measured in intermediate-aged stands follow an age-related decrease in productivity that has been reflected in standard forestry yield tables for centuries (Gower et al. 1996). However, our intermediate-aged stands are plantations that were generated following harvesting, whereas the mature conifer stands were fire generated. This complicates some of the relationships, but it is typical of the mosaic of the southern Canadian forest, where harvesting has had considerable influence over the past five decades.

Ryan et al. (1997) gave several possible reasons for decreased gross primary productivity (GPP) and NPP with stand development. Decreased leaf area due to tree mortality,

Fig. 5. August 2003 (*a*) light use efficiency (ε), calculated using incident PAR flux (Q_i); and (*b*) water use efficiency index, calculated as the ratio of mean GEP_{day} to E_{day}, for individual forest sites versus age since disturbance (or planting) and for peatland sites (far right).

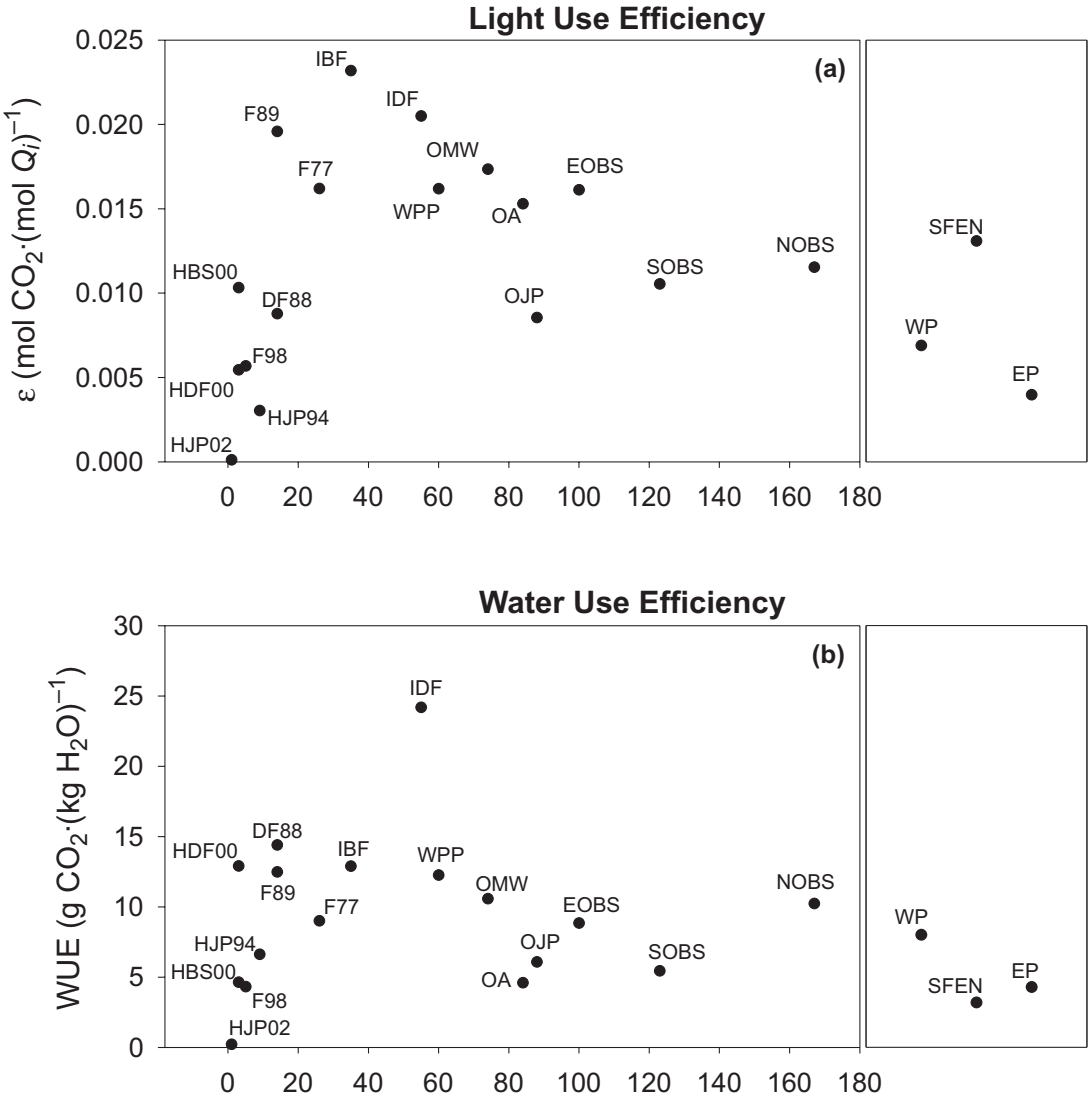

increasing hydrological constraints with increasing branch length, changes in C allocation to growth and respiration, and decreases in nutrient supply have all been suggested as possibilities. Indeed, multiple factors may be active on a single site at a given stage of development. An experimental test with *Eucalytpus* plantations in Hawaii indicated that GPP declined with stand age, whereas the belowground allocation of GPP and the fraction partitioned to foliar respiration increased (Ryan et al. 2004). Unraveling the mechanistic reasons for trends in GEP_{max}, R_{eco}, and NEP_{max} will be a key topic to be addressed as additional ecological data become available to the network.

Fire versus harvest

The current study examines both fire and harvest as agents of stand renewal. Over the past few decades, 2×10^6 to 3×10^6 ha of forest has burned annually (Stocks et al. 2002), whereas about 1×10^6 ha·year^{-1} has been harvested (CCFM 1997). Fire releases large amounts of C to the atmosphere during direct combustion, averaging about 27 Tg C·year^{-1} in Canada over the past four decades (Amiro et al. 2001). In contrast, harvest removes wood products that are used in a variety of ways. Some differences between fire and harvesting may be related to site factors, such as soil type and hydrology. However, fire and harvest are also fundamentally different because fire removes the fine organic material during combustion, leaving the coarse material, whereas harvesting does exactly the opposite. Fire sites F89 and F77 had much higher respiration rates than the harvested sites (see Fig. 3*c*), most likely because decaying coarse woody debris left after the fires contributed large amounts of heterotrophic respiration. It is logical to hypothesize that harvested sites would reach their highest NEP of the successional sequence sooner than naturally disturbed sites because harvesting removes the coarse woody debris that would otherwise provide a long-lasting source of heterotrophic CO_2.

Another important difference between fire and harvest as disturbance agents is that the successional trajectory and species are often different following fire. For most of our harvested sites, regeneration was controlled through mono-

Fig. 6. August 2003 (*a*) mean total daytime water flux (kg $H_2O \cdot m^{-2} \cdot day^{-1}$) and (*b*) evaporative fraction, calculated when the mean Q_i for a given 30 min period was greater than 5 $\mu mol \cdot m^{-2} \cdot s^{-1}$, for individual forest sites versus age since disturbance (or planting) and for peatland sites (far right). EF was not calculated for HJP02 and SFEN because $R_{n\text{-}day}$ was not available.

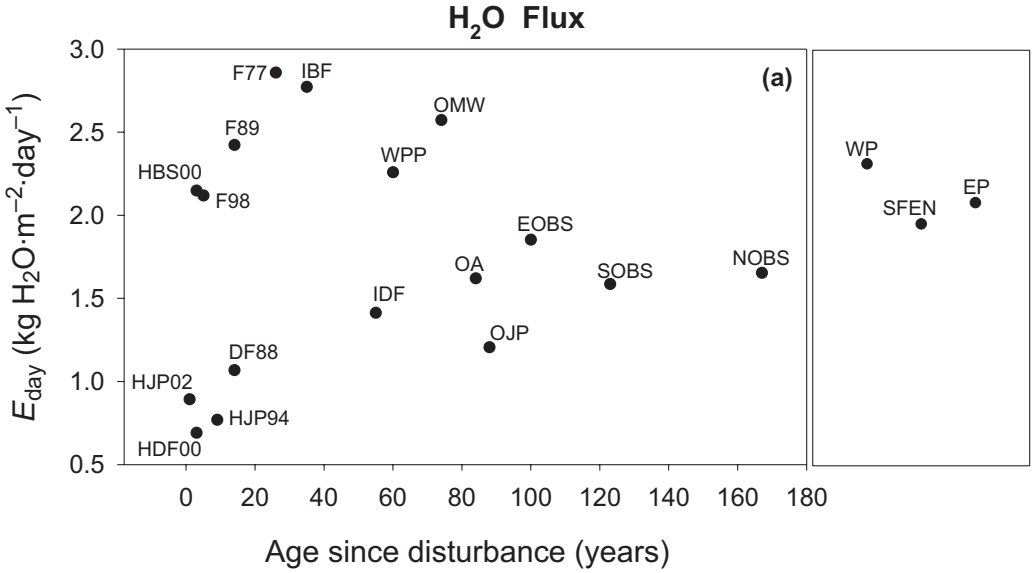

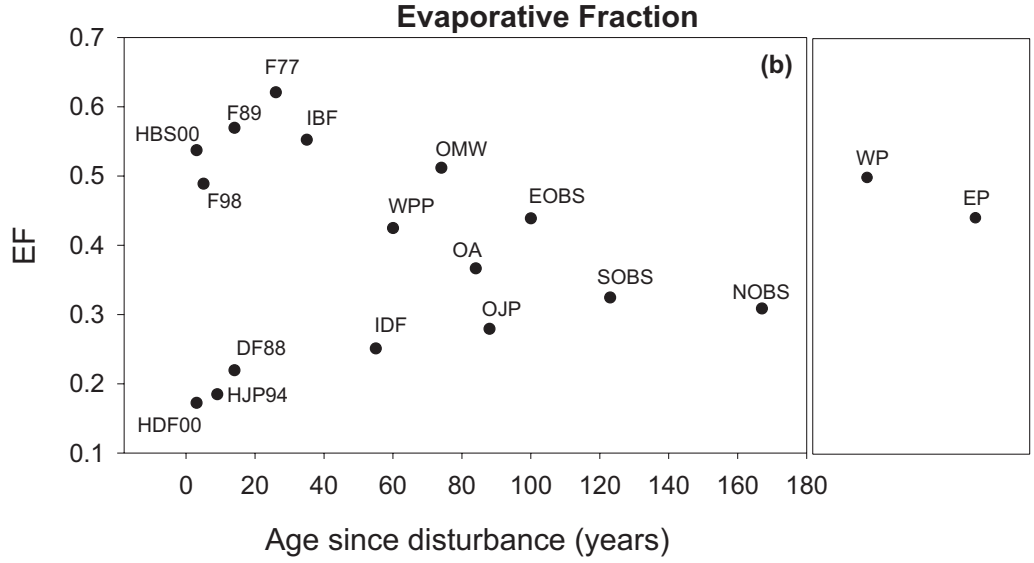

specific planting. Our fire sites, on the other hand, were naturally regenerated and have greater species diversity because of aspen sprouting and the release of serotinous seeds of jack pine and black spruce. The presence of both coniferous and deciduous species on the fire sites is the likely reason for the NEP being higher there than on the younger harvested conifer sites (see Figs. 2 and 3). The strength of our measurements of young postfire and postharvest forests is that we are bracketing the range of fluxes that are possible across the continent. Interestingly, despite different environments and species assemblages, time since disturbance explains a good portion of the observed differences in NEP.

Peatlands

Although peatlands occupy considerably less area than forests, the peatland C pool is usually many times greater than the forest C pool, and this is one reason that peatlands are an important element of our network. The results presented here indicate that C exchange varied between the peatland sites, with the largest fluxes (day and night) found at fen site WP (Figs. 2 and 3). This difference may be climate related (the western site was cooler than sites EP and SFEN in August 2003), or it may be the result of differences in vegetation. The low fluxes measured for site SFEN seem to reflect the effects of drought on GEP, but the influence of R_{eco} was less clear (Fig. 3).

Sites WP, EP, and SFEN vary in a number of respects that could have influenced NEP during August 2003. First, site EP is a bog with water and nutrient inputs to the ecosystem coming from precipitation, and site WP is a fen that receives additional inputs of nutrients from groundwater inflow (Vitt et al. 1995). Site SFEN, on the other hand, is a patterned fen

characterized by alternating strings of higher, drier areas and lower, wetter areas, both of which are oriented perpendicular to the hydrologic flow (Suyker et al. 1997). The water table is higher at site WP than at site EP. The differences in depth to water table can affect a number of ecological processes, including photosynthesis, respiration, and decomposition, which will be reflected in the C exchange measured by EC (Joiner et al. 1999; Lafleur et al. 2003). As well, it appears that there are significant differences in the amount of live aboveground biomass between sites, and this can have a significant effect on GEP and R_{eco} in peatlands.

Ecosystem-level resource use efficiency

Patterns of light use efficiency (ε) based on incident PAR versus age since disturbance (see Fig. 5) were similar to the patterns for NEP_{max}, GEP_{max}, and R_{eco} (see Fig. 3), although, as was the case for R_{eco}, values of ε for sites F77 and F89 tended to be higher. When the fraction of absorbed PAR (fPAR) product based on 5 km × 5 km moderate resolution imaging spectroradiometer (MODIS) reflectances was used to calculate ε on the basis of absorbed PAR and GEP_{max}, the same general pattern of ε with age occurred (data not shown). Light use efficiency is a critical parameter in many of the large-scale, bottom-up C cycle models that use remote sensing inputs (e.g., Heinsch et al. 2003; Running et al. 2004). Its maximum value is currently set for a biome and then modulated downward as a function of environmental stress. The maximum ε values used in the MODIS algorithm for GPP for forests range between 0.021 and 0.026 mol CO_2·(mol absorbed PAR)$^{-1}$ (Heinsch et al. 2003). These values are consistent with our upper levels of ε based on incident PAR (Fig. 5). Martel et al. (2005) and Turner et al. (2003) have shown that site-specific values of ε determined from flux tower measurements in boreal forests can differ significantly from those calculated from the MODIS algorithm for GPP. Varying the maximum ε values as a function of seral stage could add greater precision to these types of C cycle models.

Our WUE index (GEP_{day}/LE_{day}) does not differentiate between evaporation and transpiration and thus it is not the equivalent of WUE as it is commonly used in physiological studies. Nevertheless, it does give a good indication of the ratio of C absorption by an ecosystem to its water flux to the atmosphere. Results indicated that recently disturbed forests tended to have lower WUE than other forests, except in the case of site HDF00 (Fig. 5*b*). In general, the Douglas-fir sites had higher WUE and lower LE_{day} values than the other sites in their respective ecosystem categories. This was likely due to the strong drought that habitually occurs during August in this region of Canada. Similarly, the low WUE at site OA relative to the values at the other mature deciduous and conifer sites (Fig. 5*b*) was likely related to the strongly reduced canopy conductance, photosynthesis, and productivity at site OA in 2003, the third consecutive year of abnormally low rainfall (Barr et al. 2004; Hogg et al. 2005). The low E_{day} and EF values at conifer-dominated, recently disturbed sites in western Canada (see Fig. 6) indicate the potential for significant feedback of disturbance on water flux to the planetary boundary layer, with consequent effects on cloud dynamics (Betts 2004). The E_{day} and EF values remained high on sites HBS00 and F98, and this could indicate that disturbance-driven atmospheric feedback may not occur in more humid eastern Canada or for sites where there is a significant hardwood component in the regenerating tree species.

Conclusion

Across the east–west continental transect of the FCRN, diurnal courses of NEP for August 2003 showed strong coherence within the different ecosystem categories. Recently disturbed sites showed the weakest diurnal cycle; sites with intermediate-aged conifers, the strongest. The western treed fen had a more pronounced diurnal pattern than the eastern shrub bog or the Saskatchewan patterned fen. All but 3 of the 20 sites were clearly afternoon C sinks. Ecosystem respiration was highest for the young fire sites, followed by the intermediate-aged conifer and mature deciduous sites. The intermediate-aged conifer sites had the highest NEP_{max} and GEP_{max}, attaining rates that would be consistent with the presence of a strong terrestrial C sink in these regions. Our results support the idea that large-scale C cycle modeling activities would benefit from information on the age-class distribution within larger grid cells.

Ecosystem light use efficiency (ε) followed a pattern similar to those for NEP_{max} and GEP_{max}, with the intermediate-aged balsam fir having the highest values. Varying the biome-level ε values as a function of seral stage could add greater precision to the regional and global C cycle models that are based on light use efficiency. The low E_{day} and EF values for the conifer-dominated, recently disturbed sites in western Canada indicate the potential for significant feedback of disturbance on water flux to the planetary boundary layer, with consequent effects on cloud dynamics. On the other hand, E_{day} and EF values were high on the recently harvested site in eastern Canada and on the mixed conifer–hardwood 1998 fire site in Saskatchewan. This suggests that this type of disturbance-driven atmospheric feedback may not occur in more humid regions of Canada or for sites having a significant hardwood component.

FCRN provides the site-level process measurements and analyses needed for an understanding of what might be expected as the age-class structure of Canadian forests changes over the coming decades under a potentially changing climate. When these analyses are combined with remote sensing of land surface biophysical properties, forest inventory information, atmospheric trace gas measurements, and ecosystem process models, we can provide defensible estimates of the role of climate and disturbance in the C cycle of Canada.

Acknowledgements

Funding to Canadian universities was provided by the Canadian Foundation for Climate and Atmospheric Sciences, the Natural Sciences and Engineering Research Council of Canada, and the BIOCAP Canada Foundation. Funding to Canadian government scientists was provided by Natural Resources Canada and the Meteorological Service of Canada, with contributions from the Program of Energy Research and Development and Action Plan 2000. Funding for work at the NOBS site was provided by NASA's Terrestrial Ecol-

ogy Program. We thank Anne Larcher and Marc-André Giasson for their assistance with data analysis.

References

Amiro, B.D., Todd, J.B., Wotton, B.M., Logan, K.A., Flannigan, M.D., Stocks, B.J., Mason, J.A., Martell, D.L., and Hirsch, K.G. 2001. Direct carbon emissions from Canadian forest fires, 1959–1999. Can. J. For. Res. **31**: 512–525.

Amiro, B.D., Barr, A.G., Black, T.A., Iwashita, H., Kljun, N., McCaughey, J.H., Morgenstern, K., Murayama, S., Nesic, Z., Orchansky, A.L., and Saigusa, N. 2006. Carbon, energy and water fluxes at mature and disturbed forest sites, Saskatchewan, Canada. Agric. For. Meteorol. In press.

Arain, M.A., and Restrepo-Coupe, N. 2005. Net ecosystem production in a temperate pine plantation in southeastern Canada. Agric. For. Meteorol. **128**: 223–241.

Baldocchi, D.D. 1997. Flux footprints within and over forest canopies. Boundary-Layer Meteorol. **85**: 273–292.

Baldocchi, D.D. 2003. Assessing the eddy covariance technique for evaluating carbon dioxide exchange rates of ecosystems: past, present and future. Global Change Biol. **9**: 479–492.

Baldocchi, D.D., Vogel, C.A., and Hall, B. 1997. Seasonal variation of carbon dioxide exchange rates above and below a boreal jack pine forest. Agric. For. Meteorol. **83**: 147–170.

Barr, A.G., Black, T.A., Hogg, E.H., Kljun, N., Morgenstern, K., and Nesic, Z. 2004. Inter-annual variability in the leaf area index of a boreal aspen–hazelnut forest in relation to net ecosystem production. Agric. For. Meteorol. **126**: 237–255.

Battle, M., Bender, M.L., Tans, P.P., White, J.W.C., Ellis, J.T., Conway, T., and Francey, R.J. 2000. Global carbon sinks and their variability inferred from atmospheric O_2 and $\delta^{13}C$. Science (Washington, D.C.), **287**: 2467–2470.

Betts, A.K. 2004. Understanding hydrometeorology using global models. Bull. Am. Meteorol. Soc. **85**: 1673–1688.

Bond-Lamberty, B., Wang, C., and Gower, S.T. 2004. Net primary production and net ecosystem production of a boreal black spruce wildfire chronosequence. Global Change Biol. **10**: 473–487.

Bousquet, P., Peylin, P. Ciais, P., Le Quéré, C., Friedlingstein, P., and Tans, P. 2000. Regional changes in carbon dioxide fluxes of land and oceans since 1980. Science (Washington, D.C.), **290**: 1342–1346.

CCFM (Canadian Council of Forest Ministers). 1997. Compendium of Canadian forestry statistics 1996. Canadian Council of Forest Ministers, Natural Resources Canada, Ottawa, Ont.

Chen, J.M., Chen, W.J., Lui, J., Cihlar, J., and Gray, S. 2000. Annual carbon balance of Canada's forests during 1895–1996. Global Biogeochem. Cycles, **14**: 839–850.

Chen, J., Falk, M., Euskirchen, E., Paw U, K.T., Suchanek, T.H., Ustin, S.L., Bond, B.J., Brosofske, K.D., Phillips, N., and Bi, R. 2002*a*. Biophysical controls of carbon flows in three successional Douglas-fir stands based on eddy-covariance measurements. Tree Physiol. **22**: 169–177.

Chen, W.J., Chen, J.M., Price, D.T., and Cihlar, J. 2002*b*. Effects of stand age on net primary productivity of boreal black spruce forests in Ontario, Canada. Can. J. For. Res. **32**: 833–842.

Cihlar, J., Guindon, B., Beaubien, J., Latifovic, R., Peddle, D., Wulder, M., Fernandes, R., and Kerr, J. 2003. From need to product: a methodology for completing a land cover map of Canada with Landsat data. Can. J. Remote Sens. **29**: 171–186.

Cohen, W.B., and Goward, S.N. 2004. Landsat's role in ecological applications of remote sensing. Bioscience, **54**: 535–545.

Ecoregions Working Group. 1989. Ecological land classification series, No. 23. Canada Committee on Ecological Land Classification. Sustainable Development Branch, Canadian Wildlife Service, Environment Canada, Ottawa, Ont.

Falge, E., Baldocchi, D., Olson, R., Anthoni, P., Aubinet, M., Bernhofer, C., Burba, G., Ceulemans, R., Clement, R., Dolman, H., Granier, A., Gross, P., Grünwald, T., Hollinger, D., Jensen, N.-O., Katul, G., Keronen, P., Kowalski, A., Ta Lai, C., Law, B.E., Meyers, T., Moncrieff, J., Moors, E., Munger, J.W., Pilegaar, K., Rannik, Ü. Rebmann, C., Suyker, A., Tenhunen, J., Tu, K., Verma, S., Valasa, T., Wilson, K., and Wofsy, S.C. 2001. Gap filling strategies for defensible annual sums of net ecosystem exchange. Agric. For. Meteorol. **107**: 43–69.

Fan, S., Gloor, M., Mahlman, J., Pacala, S., Sarmiento, J., Takahashi, T., and Tans, P. 1998. A large terrestrial carbon sink in North America implied by atmospheric and oceanic carbon dioxide data and models. Science (Washington, D.C.), **282**: 442–446.

Foster, D.R., and Aber, J.D. (*Editors*). 2004. Forests in time: the environmental consequences of 1,000 years of change in New England. Yale University Press, New Haven, Conn.

Global Carbon Project. 2003. Science framework and implementation. Report 1. Earth System Science Partnership (IGBP, IHDP, WCRP, DIVERSITAS) – Global Carbon Project, Canberra, Australia.

Goulden, M.L., Munger, J.W., Fan, S., Daube, B.C., and Wofsy, S.C. 1996. Measurements of carbon sequestration by long-term eddy covariance: methods and a critical evaluation of accuracy. Global Change Biol. **2**: 169–182.

Gower, S.T., McMurtrie, R.E., and Murty, D. 1996. Aboveground net primary production decline with stand age: potential causes. Trees (Berl.), **11**: 378–382.

Griffis, T.J., Black, T.A., Morgenstern, K., Barr, A.G., Nesic, Z., Drewitt, G.B., Gaumont-Guay, D., and McCaughey, J.H. 2003. Ecophysiological controls on the carbon balances of three southern boreal forests. Agric. For. Meteorol. **117**: 53–71.

Gurney, K.B., Law, R.M., Denning, A.S., Rayner, P.J., Baker, D., Bousquet, P., Bruhwiller, L., Chen, Y.-H., Ciais, P., Fan, S., Fung, I.Y., Gloor, M., Heimann, M., Higuchi, K., John, J., Maki, T., Maksyutov, S., Masarie, K., Peylin, P., Prather, M., Pak, B.C., Randerson, J., Sarmiento, J., Taguchi, S., Takahashi, T., and Yuen, C.W. 2002. Towards robust regional estimates of CO_2 sources and sinks using atmospheric transport models. Nature (London), **415**: 626–630.

Heinsch, F.A., Reeves, M., Bowker, C.F., Votava, P., Kang, S., Milesi, C., Zhao, M., Glassy, J., Jolly, W.M., Kimball, J.S., Nemani, R.R., and Running, S.W. 2003. User's guide: GPP and NPP (MOD17A2/A3) products. NASA MODIS land algorithm. Version 1.3. Available from http://www.ntsg.umt.edu/modis/MOD17UsersGuide.pdf [accessed 20 March 2005].

Hogg, E.H., Brandt, J.P., and Kochtubajda, B. 2005. Factors affecting interannual variation in growth of western Canadian aspen forests during 1951–2000. Can. J. For. Res. **35**: 610–622.

Houghton, R.A. 2003. Why are estimates of terrestrial carbon balance so different? Global Change Biol. **9**: 500–509.

Howard, E.A., Gower, S.T., Foley, J.A., and Kucharik, C.J. 2004. Effects of logging on carbon dynamics of a jack pine forest in Saskatchewan. Global Change Biol. **10**: 1267–1284.

IPCC. 2001. Climate change 2001: the scientific basis. Contribution of Working Group I to the Third Assessment Report of the Intergovernmental Panel on Climate Change. Cambridge University Press, Cambridge, UK.

Joiner, D.W., Lafleur, P.M., McCaughey, J.H., and Bartlett, P.A. 1999. Interannual variability in carbon dioxide exchanges at a boreal wetland in the BOREAS northern study area. J. Geophys. Res. **D22**: 27 663 – 27 672.

Kurz, W.A., and Apps, M.J. 1999. A 70-year retrospective analysis of carbon fluxes in the Canadian forest sector. Ecol. Appl. **9**: 526–547.

Lafleur, P.M., Roulet, N.T., Bubier, J.L., Frolking, S., and Moore, T.R. 2003. Interannual variability in the peatland–atmosphere carbon dioxide exchange at an ombrotrophic bog. Global Biogeochem. Cycles, **17**(2): 1036. doi: 10.1029/2002GB001983.

Landsberg, J.J. 1977. Some useful equations for biological studies. Exp. Agric. **13**: 272–286.

Litvak, M., Miller, S., Wofsy, S.C., and Goulden, M.L. 2003. Effect of stand age on whole ecosystem CO_2 exchange in the Canadian boreal forest. J. Geophys. Res. **108**(D3): 8225. doi: 10.1029/2001JD000854.

Martel, M.-C., Margolis, H.A. Coursolle, C., Bigras, F.J., Heinsch, F.A., and Running, S.W. 2005. Decreasing photosynthesis at different spatial scales during the late growing season on a boreal cutover. Tree Physiol. **25**: 689–699.

Martin, J.L., Gower, S.T., Plaut, J., and Holmes, B. 2005. Carbon pools in a boreal mixedwood logging chronosequence. Global Change Biol. 11: 1883–1894.

Masek, J., Shock, C.T., and Goward, S.N. 2001. Research environment for advanced Landsat monitoring (REALM): a computational approach for Landsat-7 global science. Remote Sens. Environ. **78**: 204–216.

Morgenstern, K., Black, T.A., Humphreys, E.R., Griffis, T.J., Drewitt, G.B., Cai, T., Nesic, Z., Spittlehouse, D.L., and Livingston, N.J. 2004. Sensitivity and uncertainty of the carbon balance of a Pacific Northwest Douglas-fir forest during an El Niño/La Niña cycle. Agric. For. Meteorol. **123**: 201–219.

NRCan. 2003. Atlas of Canada. Natural Resources Canada. Available from http://atlas.gc.ca/site/english/maps/environment/forest/forestcanada/terrestrialecozones [accessed 15 August 2004].

Pacala, S.W., Hurtt, G.C., Baker, D., Peylin, P., Houghton, R.A., Birdsey, R.A., Heath, L., Sundquist, E.T., Stallard, R.F., Ciais, P., Moorcroft, P., Caspersen, J.P., Shevliakova, E., Moore, B., Kohlmaier, G., Holland, E., Gloor, M., Harmon, M.E., Fan, S.-M., Sarmiento, J.L., Goodale, C.L., Schimel, D., and Field, C.B. 2001. Consistent land- and atmosphere-based U.S. carbon sink estimates. Science (Washington, D.C.), **292**: 2316–2320.

Pregitzer, K.S., and Euskirchen, E.S. 2004. Carbon cycling and storage in world forests: biome patterns related to forest age. Global Change Biol. **10**: 1–26.

Rödenbeck, C., Houweling, S., Gloor, M., and Heimann, M. 2003. CO_2 flux history 1982–2001 inferred from atmospheric data using a global inversion of atmospheric transport. Atmos. Chem. Phys. **3**: 1919–1964.

Running, S.W., Baldocchi, D.D., Turner, D.P., Gower, S.T., Bakwin, P.S., and Hibbard, K.A. 1999. A global terrestrial monitoring network integrating tower fluxes, flask sampling, ecosystem modeling and EOS satellite data. Remote Sens. Environ. **70**: 108–127.

Running, S.W., Nemani, R.R., Heinsch, F.A., Zhao, M., Reeves, M., and Hashimoto, H. 2004. A continuous satellite-derived measure of global terrestrial primary production. Bioscience, **54**: 547–560.

Ryan, M.G., Binkley, D., and Fownes, J.H. 1997. Age-related decline in forest productivity: pattern and process. Adv. Ecol. Res. **27**: 213–261.

Ryan, M.G., Binkley, D., Fownes, J.H., Giardina, C.P., and Senock, R.S. 2004. An experimental test of the causes of forest growth decline with stand age. Ecol. Monogr. **74**: 393–414.

Sarmiento, J.L., and Gruber, N. 2002. Sinks for anthropogenic carbon. Phys. Today, **55**(8): 30–36.

Schuepp, P.H., Leclerc, M.Y., MacPherson, J.I., and Desjardins, R.L. 1990. Footprint prediction of scalar fluxes from analytical solutions of the diffusion equation. Boundary-Layer Meteorol. **50**: 355–373.

Stocks, B.J., Mason, J.A., Todd, J.B., Bosch, E.M., Wotton, B.M., Amiro, B.D., Flannigan, M.D., Hirsch, K.G., Logan, K.A., Martell D.L., and Skinner, W.R. 2002. Large forest fires in Canada, 1959–1997. J. Geophys. Res. **107**: 8149. doi: 10.1029/2001JD000484.

Suyker, A.E., Verma, S.B., and Arkebauer, T.J. 1997. Season-long measurement of carbon dioxide exchange in a boreal fen. J. Geophys. Res. **102**(D24): 29 021–29 028.

Tanner, C.B., and Thurtell, G.W. 1969. Sensible heat flux measurements with a yaw sphere and thermometer. Report TR Ecom 66-G22-F. University of Wisconsin, Madison, Wis.

Thompson, M.V., Randerson, J.T., Malmström, C.M., and Field, C.B. 1996. Change in net primary production and heterotrophic respiration: How much is necessary to sustain the terrestrial carbon sink? Global Biogeochem. Cycles **10**: 711–726.

Turner, D.P., Ritts, W.D., Cohen, W.B., Gower, S.T., Zhao, M., Running, S.W., Wofsy, S.C., Urbanski, S., Dunn, A., and Munger, J.W. 2003. Scaling gross primary production (GPP) over boreal and deciduous forest landscapes in support of MODIS GPP product validation. Remote Sens. Environ. **88**: 256–270.

Vitt, D.H, Bayley, S.E., and Jin, T.-L. 1995. Seasonal variation in water chemistry over a bog-rich fen gradient in Continental Western Canada. Can. J. Fish. Aquat. Sci. **52**: 587–606.

Webb, E.K., Pearman, G.I., and Leuning, R. 1980. Correction of flux measurements for density effects due to heat and water vapor transfer. Q. J. R. Meteorol. Soc. **106**: 85–100.

Wirth, C., Czimczik, C., and Schulze, E.-D. 2002. Beyond annual budgets: carbon flux at different temporal scales in fire-prone Siberian Scots pine plantations. Tellus, **54B**: 611–630.

Wofsy, S. 2004. The Harvard Forest and understanding the global carbon budget. *In* Forests in time: the environmental consequences of 1,000 years of change in New England. *Edited by* D.R. Foster and J.D. Aber. Yale University Press, New Haven, Conn. pp. 380–393.

List of symbols

α	quantum efficiency parameter of a light response curve (mol CO_2·(mol PAR)$^{-1}$)
Γ	light compensation point (μmol PAR·m^{-2}·s^{-1})
ε	daily average ecosystem light use efficiency (mol CO_2·(mol PAR)$^{-1}$) for August 2003
E_{day}	mean total daytime H_2O flux (kg·m^{-2}·day^{-1}) for August 2003
EF	mean evaporative fraction ($LE_{day}/R_{n\text{-}day}$) for August 2003
F_c	above-canopy flux (μmol CO_2·m^{-2}·s^{-1})
GEP_{day}	daily gross ecosystem productivity (μmol CO_2·m^{-2}·day^{-1}) for August 2003
GEP_{max}	maximum gross ecosystem productivity (μmol CO_2·m^{-2}·s^{-1})
GPP	gross primary productivity
LE_{day}	mean total daytime water (latent energy) flux (J·m^{-2}·day^{-1}) for August 2003
NEE	net ecosystem exchange (μmol CO_2·m^{-2}·s^{-1})
NEP	net ecosystem productivity (μmol CO_2·m^{-2}·s^{-1})
NEP_{max}	maximum net ecosystem productivity (μmol CO_2·m^{-2}·s^{-1})
NPP	net primary productivity
PAR	photosynthetically active radiation
Q_i	flux of incident photosynthetically active radiation (μmol PAR·m^{-2}·s^{-1})
Q_{day}	mean total daytime flux of incident photosynthetically active radiation (mol PAR·m^{-2}·day^{-1}) for August 2003

R_{day} mean total daytime respiration (μmol $CO_2 \cdot m^{-2} \cdot day^{-1}$) for August 2003
R_{eco} mean ecosystem respiration (μmol $CO_2 \cdot m^{-2} \cdot s^{-1}$) for August 2003
$R_{n\text{-}day}$ mean total daytime net radiation ($J \cdot m^{-2} \cdot day^{-1}$) for August 2003
S CO_2 storage in the air column below the flux sensors (μmol $CO_2 \cdot m^{-2} \cdot s^{-1}$)
t time (s)
u_* friction velocity ($m \cdot s^{-1}$)
WUE water use efficiency (g $CO_2 \cdot (kg\ H_2O)^{-1}$)